ISSN 0915-633X

NATIONAL INSTITUTE FOR FUSION SCIENCE

Q-profile Flattening due to Nonlinear Development of Resistive Kink Mode and Ensuing Fast Crash in Sawtooth Oscillations

K. Watanabe, T. Sato and Y. Nakayama

(Received – July 28, 1993)

NIFS-238 July 1993

RESEARCH REPORT
NIFS Series

NAGOYA, JAPAN

Q-profile Flattening due to Nonlinear Development of Resistive Kink Mode and Ensuing Fast Crash in Sawtooth Oscillations

K. Watanabe and T. Sato

National Institute for Fusion Science, Nagoya 464-01, Japan

Y. Nakayama

Canon Systems Globalization, Inc., Santa Clara 95054, U.S.A.

Keywords

tokamak, sawtooth oscillation, computer simulation, magnetohydrodynamics, magnetic reconnection

Abstract

Presented is a new full-torus, compressible, resistive MHD simulation model that can adequately explain the mechanism of the fast crash in the sawtooth oscillation. The simulation results reveal that the q value, which at first decreases in accordance with current peaking subject to ohmic heating, starts increasing in the $q < 1$ region due to strong excitation of nonlinear resistive kink modes and tends to be bottom-flattened. When the q profile is largely flattened in the $q < 1$ region, the dynamic pressure of the m=1 kink mode pushes the hot core plasma in the main flow direction and the hot core deviates from the magnetic axis. Then, a strong plasma compression occurs at the stagnation point of the directed plasma flow which is coincident with the m=1 rational surface. Consequently, the poloidal magnetic field lines are driven to reconnect rapidly with each other across the q=1 surface, and the deviated hot core is pushed out towards the wall to destroy its confinement. The driven magnetic reconnection leading to the crash is found to occur as a result of the q-profile flattening, in contrast to Kadomtsev's model where the q-profile becomes flattened as a result of reconnection exchanging the magnetic flux. The crash is governed by the MHD time scale, about 100 poloidal Alfven transit times, which is much faster than the Kadomtsev reconnection time. The resistive kink mode and its nonlinear behavior control the whole process of the sawtooth oscillation. Especially, the m=1 plasma flow induced by the resistive kink instability, neither the magnetic force nor the pressure force, plays a decisive role in triggering the crash.

I. INTRODUCTION

The mechanism of the fast crash in the sawtooth oscillation yet remains unclarified while there have been many theoretical researches reported [1–4]. In recent large tokamak experiments [5], the change in the temperature distribution in the crash phase seems to support Kadomtsev's resistive model [6] rather than Wesson's interchange mode model [7] as far as the geometrical change of the plasma is concerned, but it remains difficult to account for the rapid time scale of the fast crash.

For example, Aydemir [1] showed that the quasi-interchange mode, resistive quasi-interchange mode, and then, resistive kink mode, are excited during the ramp-up phase and that the crash is caused by the resistive kink mode. The time-scale of the crash obtained in his work, however, is much longer than the time-scale observed in the experiments. In order to get faster time-scale of the crash, it has recently been proposed that collisionless m=1 modes exhibit nonlinearly enhanced growth rates in high temperature plasmas [8,9]. Especially, when an adiabatic electron response is allowed, it leads to an abrupt increase in the growth rate and thus in the reconnection rate. It is pointed out that the nonlinear increase of the reconnection rate may explain the fast sawtooth crash time.

Our aim of this study is to examine whether or not the fast sawtooth crash can be explained within the classical MHD framework where a small classical resistivity is assumed, namely, without invoking any nonlinearly enhanced resistivity. For this purpose, we have executed self-consistent three-dimensional compressible resistive MHD simulations for a torus geometry, in which we have elaborated the previous model [10] and reconstructed a more feasible simulation model representing an ohmically heated tokamak plasma. In the previous model, the assumed resistivity model was not realistic in the sense that the vacuum periphery region was represented by a very large resistive medium. Because of the existence of the highly resistive periphery region, an artificial remedy was done to

connect smoothly the core region and the periphery region.

II. SIMULATION MODEL AND RESULTS

The basic equations are

$$\frac{\partial \rho}{\partial t} + \nabla \cdot (\rho \boldsymbol{v}) = 0, \tag{1}$$

$$\rho \frac{d \boldsymbol{v}}{d t} = \boldsymbol{j} \times \boldsymbol{B} - \nabla p, \tag{2}$$

$$\frac{\partial \boldsymbol{B}}{\partial t} = \nabla \times (\boldsymbol{v} \times \boldsymbol{B}) - \nabla \times (\boldsymbol{j}/S), \tag{3}$$

$$\frac{\partial p}{\partial t} + \nabla \cdot (p \boldsymbol{v}) = (\gamma - 1)(-p \nabla \cdot \boldsymbol{v} + \boldsymbol{j}^2/S) + \kappa \Delta T, \tag{4}$$

where the magnetic Reynolds number S is classical and proportional to the 3/2 power of the temperature and the thermal conductivity coefficient κ is constant. The thermal conduction effect, $\kappa \Delta T$, is switched on only when the shift of the temperature axis from the initial plasma center becomes more than 20% of the minor radius due to the temperature crash. This treatment is made with an anticipation that some kinetic effects to activate the heat conduction would be enhanced when the local temperature gradient is increased. This term is introduced merely for recovering an axially symmetric plasma pressure profile after the crash.

The tokamak device is modeled by a torus surrounded by a conducting wall with a square cross section as shown in Fig. 1, where cylindrical coordinates (R, θ, Z) are adopted ; R is the major radius, θ the toroidal angle, and Z the vertical axis. We solved the above MHD equations using a high precision code which advances the physical quantities in time using the fourth order Runge-Kutta-Gill method and in time using the fourth order centered-difference method [11,12]. The initial equilibrium configuration without resistivity is obtained by solving the Grad-Shafranov equation under the above geometry. The toroidal β is taken to be 0.1% (very low β). The initial on-axis S value is set to be 40000 and its distribution is calculated from the temperature.

The evolutions of the magnetic field lines mapped on a poloidal plane, the q profile and the plasma flow profile on the poloidal cross section are shown in Fig. 2. The q value at the plasma center which was initially set to be 1.03 ($t = 0$; Fig. 2-(a)) gradually decreases in accordance with current peaking caused by ohmic heating. As the on-axis q value falls below 1, an m=1/n=1 resistive kink mode appears near the axis. As the q value decreases further, the excited magnetic field intensity of n=1 mode, as well as the plasma flow, becomes larger and larger. After the magnetic field of n=1 mode develops to a certain amplitude, q stops reducing its on-axis value and starts increasing in the $q < 1$ region (this time is noted as the turning point, T.P., in the paper), thus being flattened ($t = 358\tau_{pA}$: $\tau_{pA} = a/V_{pA} = R_0/V_{tA}$ denotes a poloidal Alfven transit time, where the aspect ratio R_0/a is taken to be 3. ; Fig. 2-(b)).

As time elapses, the q-profile gets more and more flattened toward $q = 1$ in the whole region of $q < 1$. During this deformation of the q profile, the amplitude of the plasma flow becomes large enough to shift the temperature axis away from the magnetic axis. Here, the plasma flow directs from axis to the right-side wall and flows back around the axis to the left-side wall. It is to be noted that no Kadomtsev type reconnection is taking place in this q-profile deformation period.

When the q-profile becomes almost flattened ($t = 480\tau_{pA}$; Fig. 2-(c)), the largely developed plasma flow pushes the magnetic surface radially outwards so that the poloidal magnetic field lines are driven to reconnect rapidly with each other across the original q=1 surface at the head point of the plasma flow [13] and the energy deposited in the region $q \leq 1$ is swiftly released to the outside region.

Consequently, the central hot plasma is pushed out beyond the q=1 region and the temperature distribution crashes ($t = 484\tau_{pA}$; Fig. 2-(d)). Some poloidal Alfven transit times after the disruption, the poloidal magnetic surface tends to return to the initial axially symmetric configuration, while the pressure profile and the temperature profile

still keep collapsing ($t = 496\tau_{pA}$; Fig. 2-(e)).

In Fig. 3, the equi-contours of the temperature at (a) t=0, (b) t=358 τ_{pA}, (c) t=480 τ_{pA}, (d) t=484 τ_{pA}, (e) t=496 τ_{pA} corresponding to Fig. 2, and at (f) t=520 τ_{pA} are shown. Top panels correspond to the ramp-up phase and bottom panels to the crash phase. The temperature axis stays at its initial position for most part of the ramp-up phase (Fig. 3-(a) and (b)). At a time just before the magnetic surface disruption (Fig. 3-(c)), one can see that the temperature axis has already considerably shifted, though the magnetic axis still remains almost at the same position. In order to make visible this discrepancy between the magnetic axis and temperature axis, the magnetic field lines mapped on a poloidal plane along with the temperature distribution are drawn in Fig. 4, where the color changes from blue to red as the temperature increases.

This is due to the fact that the strong kink flow has pushed the plasma towards the wall, keeping a dynamic equilibrium where the magnetic pressure is almost in balance with the plasma dynamic pressure. The obvious discrepancy between the magnetic surface and the temperature contour can be explained by a slight imbalance between the magnetic and dynamic pressures which are much larger than the static plasma pressure. Such a shift of the temperature axis may well explain the so-called precursor of the sawtooth crash in a rotating plasma. When a crash occurs, the high temperature spot in the central region slides rapidly towards the wall, leaving a temperature plateau in the central region (Fig. 3-(f)). Invasion of cold bubbles into the hot plasma region was not observed through the whole process of the sawtooth oscillation. These features are in good agreement with observations in experiments such as TFTR. [5,14]

It should be noticed that the time span of the ramp-up phase (top panels) is 480 τ_{pA}, while that of the crash phase (bottom panels) is 36 τ_{pA}. This indicates that the crash occurs in a quite fast time-scale. Actually, as can be seen in Fig. 5 where the on-axis temperature is plotted against time, the temperature on the plasma axis drops in the

time-scale of the order of 100 τ_{pA}. Thus, the time-scale of the temperature crash is of the order of the MHD time-scale which is much faster than the resistive time-scale, and agrees with the experimental observation.

At t=532 τ_{pA}, the thermal conduction effect is switched on in the present simulation to remove the hot spot. Then, the pressure and density profiles tend to return to the initial axi-symmetric ones. Returning to the initial state of the pressure profile is completed at t=586 τ_{pA} and then, the thermal conduction is switched off. The system enters into the second ramp-up phase and a similar sawtooth feature is repeated. In the present MHD study, the heat release mechanism can not be specified, but it certainly plays an essential role in retrieving the normal state form the crash phase.

Fig. 6 shows the time development of (a) the magnetic field energy and (b) kinetic energy of the n=1 mode and the nonlinear modes. When the system reaches to the turning point of the on-axis q value (T.P.) where the on-axis q value changes from decrease to increase in the ramp-up phase, one can see that nonlinearly excited higher modes have grown drastically. The time when both of the n=1 mode and nonlinear modes ($n \geq 2$) become maximum, i.e., $t = 504\tau_{pA}$, corresponds to the time just after the magnetic surface disruption. (see Fig. 2-(e)).

III. DISCUSSIONS

A. What leads to the q-profile flattening ?

First of all, in order to identify the characteristics of the unstable mode which is shown in Fig. 6, we made several simulations with different S numbers in which the on-axis q value is fixed to be 0.85 initially. The linear growth rate obtained in these simulations are shown in Fig. 7. In this figure, the theoretical growth rate of the resistive kink mode, being proportional to $S^{-1/3}$, is indicated by the solid line [15] . The observed growth rates

show a good agreement with the $S^{-1/3}$ curve, hence, it can be confirmed that the excited mode in these simulations is the resistive kink mode, not the tearing mode whose growth rate is proportional to $S^{-3/5}$.

Fig. 8 and Fig. 9 show the time developments of the magnetic field energy and kinetic energy of n=1 mode and nonlinear modes, respectively, (a) for the case that the n=1 mode was artificially suppressed at a time before the system reached to the turning point (T.P.), (b) for the case that the n=1 mode was suppressed just before the q profile was flattened, and (c) for the original case shown in Fig. 6. In both cases (a) and (b) the on-axis q value continues to decrease for a while after the suppression of the n=1 mode. After the passage of a certain time, say, 110 τ_{pA} and 33 τ_{pA}, respectively, for the cases (a) and (b) the nonlinear modes start growing drastically again and the system reaches to the turning point. The q-profile flattening and the crash follows in the same way as the original case.

The above results indicate that the drastic growth of the nonlinear ($n \geq 2$) modes leads to the turning of the on-axis q value from decrease to increase. Namely, the excitation of nonlinear modes seems to be the very cause that leads to the lowering of the barrier protecting the disruption of the magnetic surface. In order to prove this idea, we performed an artificial simulation in which the magnetic field energy and the kinetic energy of nonlinear modes (except the primary n=1 mode) were forced to keep the levels of those values at a time before the turning point ($t = 309\tau_{pA}$). The result of this artificial simulation has shown that the q value keeps decreasing instead of being flattened, thus, no crash has occurred.

From the above studies one can conclude that the flattening of the q-profile, which leads to the crash, is caused by the strong excitation of nonlinear modes, not by the reconnection process. It is this aspect that is essentially different from Kadomtsev's model, although the overall change of the temperature profile is very similar. Namely,

in our model, the driven reconnection is triggered as a result of the q-profile flattening which is caused by the strong excitation of nonlinear modes, in contrast to Kadomtsev's model in which the q-profile becomes flattened as a result of the nonlinear reconnection exchanging the magnetic flux over q=1 surface.

B. How and what triggers the crash ?

Throughout the ramp-up phase, there occurs no violent magnetic reconnection (except for weak tearing modes). On the other hand, at the beginning of the crash phase, we can observe violent magnetic reconnection which causes the complete destruction of the magnetic surface in the $q \leq 1$ region (see Fig. 2-(d)). Such destruction of the magnetic surface leads to the crash of the pressure (temperature) profile. In the meantime, we executed a simulation in which the term $-\nabla \times (\boldsymbol{j}/S)$ was removed from Eq. (3) at a time just before the q profile was flattened. In this case, no destructive reconnection occurred, in spite of the fact that the q profile continued to be flattened. This indicates that a resistivity, whatever it may be, is necessary for triggering the crash. In this respect, a recent particle simulation has shown that when the current sheet is thinned as small as the ion Larmor radius by the compressional plasma flows, collisionless driven reconnection is rapidly induced [16]. This may imply that in a real high temperature tokamak collisionless driven reconnection may take place instead of collisional driven reconnection.

In order to assure the role of the plasma flow on magnetic reconnection in the crash phase, i.e., the role of the plasma flow in triggering the crash, we made a simulation in which only the plasma flow was artificially suppressed at a time just before the crash. The solid line in Fig. 10 indicates the time development of the kinetic energy and magnetic field energy of n=1 mode. The dashed line in the figure stands for the development of the original case. The times when the crash occurred for both cases are also shown by the arrows. It is seen that at the very beginning the kinetic energy abruptly increases so as to

retrieve a self-consistent solution by consuming a part of the magnetic field energy. When the self-consistent solution is obtained and the amplitude of the kinetic energy becomes the similar level as that of the crash time for the original case, the crash has occurred. On the other hand, the magnetic field energy at the crash time for the case where the suppression of the plasma flow was executed has reached to a higher level than that for the original case. This fact strongly supports that it is the dynamic pressure, rather than the magnetic pressure, of the n=1 kink mode that drives reconnection, hence, the fast crash. However, there still remains a question as to how the plasma pressure can contribute to triggering the crash.

In order to clarify the role of the plasma pressure in triggering the crash, we made an artificial simulation where the pressure gradient force was removed from the equation of motion, Eq. (2), just before the onset of the crash. The result was such that the crash did occur almost exactly in the same way as in the case with the pressure gradient force. Therefore, the pressure turns out not to be the major term in the sawtooth phenomena. Our final conclusion is therefore that the fast crash is directly triggered by nonlinear reconnection, whether collisional or collisionless, driven by the well-developed m=1/n=1 kink mode plasma flow.

C. What determines the scale of the crash ?

As can be seen in Figures 2 and 5, the time-scale of the disruption of the magnetic surface due to magnetic reconnection is $20 \sim 30\ \tau_{pA}$ and the temperature on the plasma axis drops in the time-scale of $50 \sim 100\ \tau_{pA}$. The difference between the time-scales of the magnetic surface disruption and the temperature drop reflects the fact that there appears an appreciable shift of the temperature axis before the crash time as is observed as a precursor in the real experiments, and also the fact that the pressure profile continues to be distorted for a while after the crash because the strongly excited kink plasma flow

cannot be damped out quickly. Although the on-axis temperature keeps decreasing after the disruption of the magnetic surface, it may be reasonable that the time-scale of the sawtooth crash is given, in a strict sense, by that of the disruption of the magnetic surface, namely, by the time-scale of magnetic reconnection.

Here, we note that in a compressible plasma the time-scale of the driven magnetic reconnection is weakly dependent on the resistivity, but dependent strongly on the magnitude of the driving plasma flow [17]. It is anticipated therefore that the time-scale of the crash will not change much, even though a higher Reynolds number is assumed, as long as the kink flow velocity is the same.

In order to see this, we executed a simulation where the initial on-axis S value is set to be 80000 which is much larger than the previous case. The on-axis temperature is plotted against time in Fig. 11. In this case, it takes about 600 τ_{pA} for the ramp up phase and 30 $\sim$ 40 τ_{pA} for the disruption of the magnetic surface. At the time when the q profile is flattened, the resistivity and the magnitude of the plasma flow velocity of the simulation for the high S case (S = 80000) is 2.3 and 1.4 times smaller than those of the original simulation with the low S case (S = 40000), respectively. This result strongly supports our anticipation that the time-scale of the disruption of the magnetic surface is determined primarily by the plasma flow velocity, rather than the resistivity.

In an incompressible plasma, the magnetic Reynolds number will affect seriously on the reconnection rate, hence, the time scale of the crash. This would give the reason why the time-scale of the crash in our simulation is different from that in the other simulations, for example, Aydemir's simulation where the density continuity equation is not solved (constant density model).

In our simulations the density variation is self-consistently taken into account, which gives an essential difference from other simulations. Particularly at the very moment of the crash, the density is narrowly peaked at the stagnation position of the directed

plasma flow, whereby strong reconnection is driven in the time-scale determined solely by the directed plasma flow.

In our simulation, the q-profile becomes flattened at q = 1 before the crash, while the actual experimental data show that the q-profile remains below q = 1 through the sawtooth oscillations. One possible explanation for this discrepancy is that the observed q-profiles in the experiments are obtained by averaging over a few sawtooth oscillation periods, therefore, the observed q-profiles may not reflect those at a time just before the crash. In our simulation, during the ramp-up phase which occupies most of the sawtooth oscillation period, the q-value is well below 1 and the q-profile flattening occurs for a short time before the crash. An another possible explanation is as follows. The key points for the crash in our model are the q-profile flattening as well as the existence of m=1/n=1 mode. Therefore, our simulation shows that during the period when the q value increases towards q=1, the bottom part of the q-profile becomes flattened at the value less than unity and the flattened region spreads as the flattened q value increases. Since in a high temperature tokamak, the S value is much larger than the present one and the growth rate of the resistive kink mode is proportional to $S^{-1/3}$, the relative growth of the resistive kink mode in the real ramp-up phase is supposed to be much larger than the present one. Therefore, it is conceivable that lower q modes. say, m/n=0.8, can be nonlinearly excited, hence, crash may occur at a bottom-flattened q-profile even if the flattened q is below 1.

The amplitude and period of the sawtooth oscillation are strongly dependent on how to remove the heat from the core region when crash occurs. However, the heat transfer mechanism must be governed by kinetic effects rather than the MHD effects. In order to explain the whole process of the sawtooth oscillation phenomena, therefore, one must wait until an innovative simulation model in which both the fluid-scale and particle-scale effects are simultaneously taken into account can be developed.

IV. SUMMARY

A comprehensive study of the fast crash mechanism of the tokamak sawtooth oscillation is done by a full-torus, compressible, resistive MHD simulation. The simulation results have concluded that the fast crash of the sawtooth oscillation can be explained within the context of the classical resistive MHD model. When the on-axis q value falls below 1, the m=1/n=1 resistive kink mode appears around the axis. As the linear kink mode grows sufficiently, the nonlinear modes are excited drastically. Then, q stops reducing its on-axis value and turns to increase so as to form a flat-bottom profile. The central hot core plasma tends to be pushed away from the rather robust magnetic axis by the dynamic pressure. When the q-profile below 1 becomes entirely flattened at q=1, the poloidal magnetic field lines are driven to reconnect rapidly in one or multiple points in the flattened q region by strong plasma flows which are induced by the kink mode, whereby the robust magnetic structure in the flattened region is crashed.

The direct cause for triggering the crash is the plasma flow which grows as a result of the kink mode. It is the driven magnetic reconnection due to this plasma flow that leads to disruption of the poloidal magnetic surface, namely, the sawtooth crash. The time-scale is governed by the MHD time-scale, say, 100 poloidal Alfven transit times.

In conclusion, the excitation of the nonlinear kink modes acts to flatten the q-profile in the unstable region and reduce the stabilizing magnetic barrier in the core region, and at the same time the growth of the kink plasma flow strengthens the force of driven magnetic reconnection, consequently, the fast crash is realized.

Acknowledgement

The authors are grateful for stimulating discussions with R. Horiuchi, T. Hayashi, and A. Y. Aydemir.

References

1. A. Y. Aydemir, J. C. Wiley, and D. W. Ross, Phys. Fluids, **B1**, 774(1989).
2. A. Y. Aydemir, Phys. Fluids, **B2**, 2135(1990).
3. W. Park, D. A. Monticello, E. Fredrickson, and K. McGuire, Phys. Fluids, **B3**, 507(1991).
4. A. J. Lichtenberg, K. Itoh, S.-I. Itoh, and A. Fukuyama, Nucl. Fusion, **32**, 495(1992).
5. Y. Nagayama, K. M. McGuire, A. Cavallo, M. Bitter, E. D. Fredrickson, K. W. Hill, H. Hsuan, A. Janos, W. Park, G. Taylor, and M. Yamada, Phys. Rev. Lett., **67**, 3527(1991).
6. B. B. Kadomtsev, Fiz. Plazmy, **1**, 710(1975) [Sov. J. Plasma Phys. **1**, 389(1975)].
7. J. A. Wesson, Plasma Phys. Controlled Fusion, **28**, 243(1986).
8. A. Y. Aydemir, Phys. Fluids, **B4**, 3469(1992).
9. X. Wang and A. Bhattacharjee, Phys. Rev. Lett., **70**, 1627(1993).
10. T. Sato, Y. Nakayama, T. Hayashi, K. Watanabe, and R. Horiuchi, Phys. Rev. Lett., **63**, 528(1989).
11. R. Horiuchi and T. Sato, Phys. Fluids, **B1**, 581(1989).
12. K. Watanabe and T. Sato, J. Geophys. Res., **95**, 75(1990).
13. T. Sato, R. Horiuchi, and K. Kusano, Phys. Fluids, **B1**, 255(1989).
14. M. Yamada, Private communications(1993).
15. B. Coppi, R. Galvao, R. Pellat, M. Rosenbluth, and P. Rutherford, Fiz. Plazmy, **2**, 961(1976) [Sov. J. Plasma Phys. **2**, 553(1976)].
16. R. Horiuchi and T. Sato, to appear in Phys. Rev. Lett.
17. T. Sato, T. Hayashi, K. Watanabe, R. Horiuchi, M. Tanaka, N. Sawairi, and K. Kusano, Phys. Fluids, **B4**, 450(1992).

Figure Captions

Fig. 1. The simulation model of the tokamak device and its coordinates system.

Fig. 2. The evolutions of magnetic field lines mapping on a poloidal plane, the q-profile and plasma flow profile at (a) t=0, (b) t=358 τ_{pA}, (c) t=480 τ_{pA}, (d) t=484 τ_{pA}, (e) t=496 τ_{pA}.

Fig. 3. The equi-contours of the temperature at (a) t=0, (b) t=358 τ_{pA}, (c) t=480 τ_{pA}, (d) t=484 τ_{pA}, (e) t=496 τ_{pA} corresponding to Fig. 2, and at (f) t=520 τ_{pA}.

Fig. 4. The magnetic field lines mapping on a poloidal plane and the temperature distribution at t=480 τ_{pA}. The color changes from blue to red as the temperature increases.

Fig. 5. The time development of the on-axis temperature. The thermal conduction effect was switched on and off at the points indicated by the vertical arrow.

Fig. 6. (a): The time development of the magnetic field energy of the n=1 mode and the nonlinear modes. (b): The time development of the plasma kinetic energy of the n=1 mode and the nonlinear modes.

Fig. 7. The growth rate of n=1 mode for different S numbers. The solid line, being proportional to $S^{-1/3}$, indicates a theoretical growth rate of the resistive kink mode.

Fig. 8. The time development of the magnetic field energy of n=1 mode, (a) for the case where the n=1 mode was artificially suppressed at a time before the turning point, (b) for the case where the n=1 mode was suppressed just before the flattening, and (c) the original case.

Fig. 9. The time development of the plasma kinetic energy of n=1 mode, (a) for the case where the n=1 mode was artificially suppressed at a time before the turning point, (b) for the case where the n=1 mode was suppressed just before

the flattening, and (c) the original case.

Fig. 10. The time developments of the kinetic energy and magnetic field energy of n=1 mode. The solid and dashed lines correspond to the case where only the plasma flow was artificially suppressed at a time just before the crash and to the original case, respectively.

Fig. 11. The time development of the on-axis temperature for the case where the initial S is taken to be 80000.

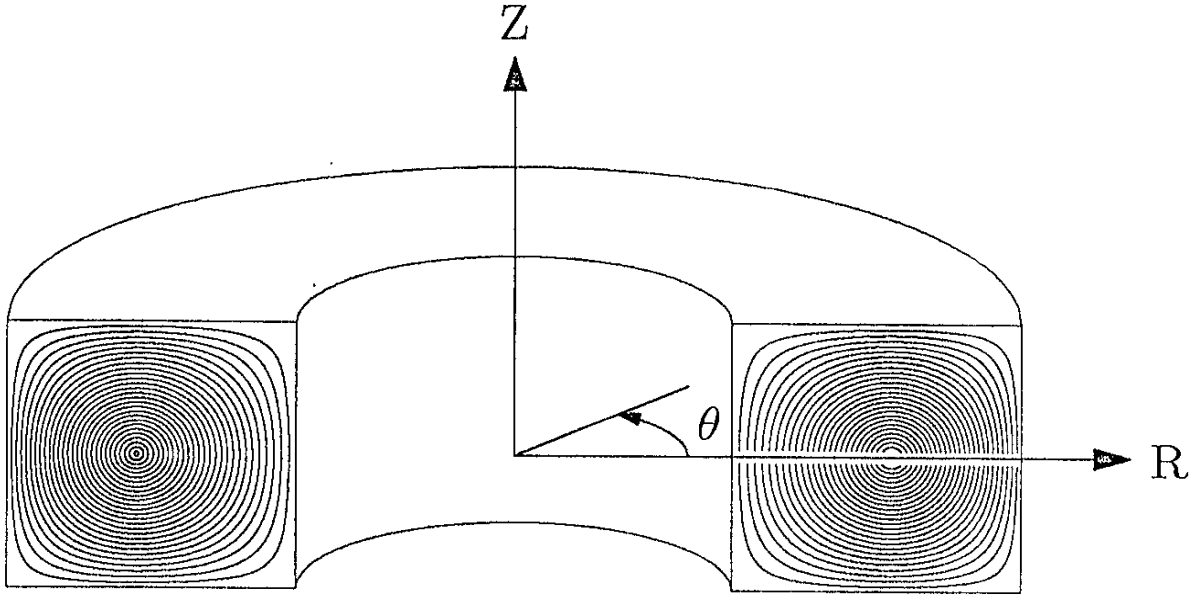

Figure 1

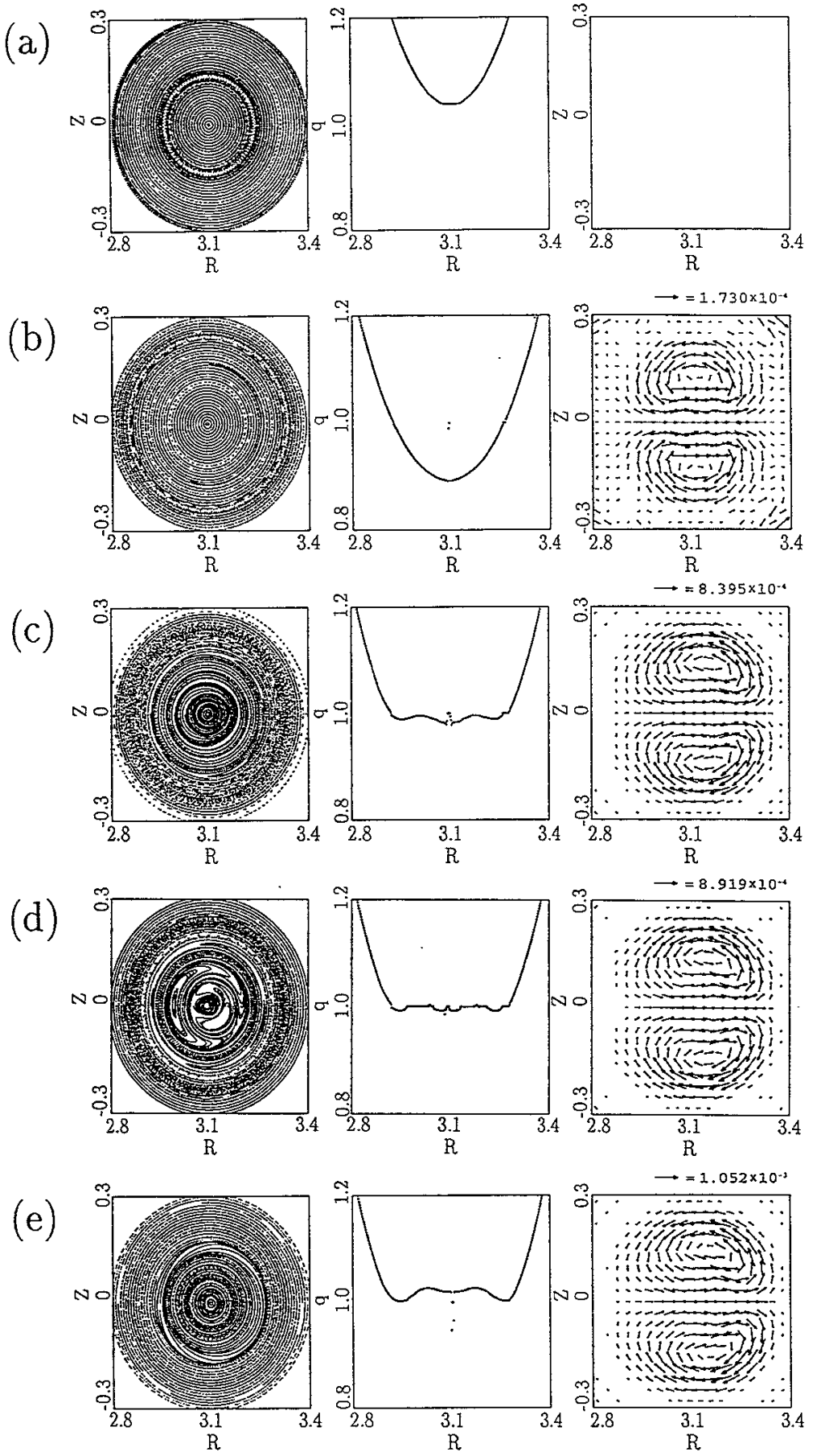

Figure 2

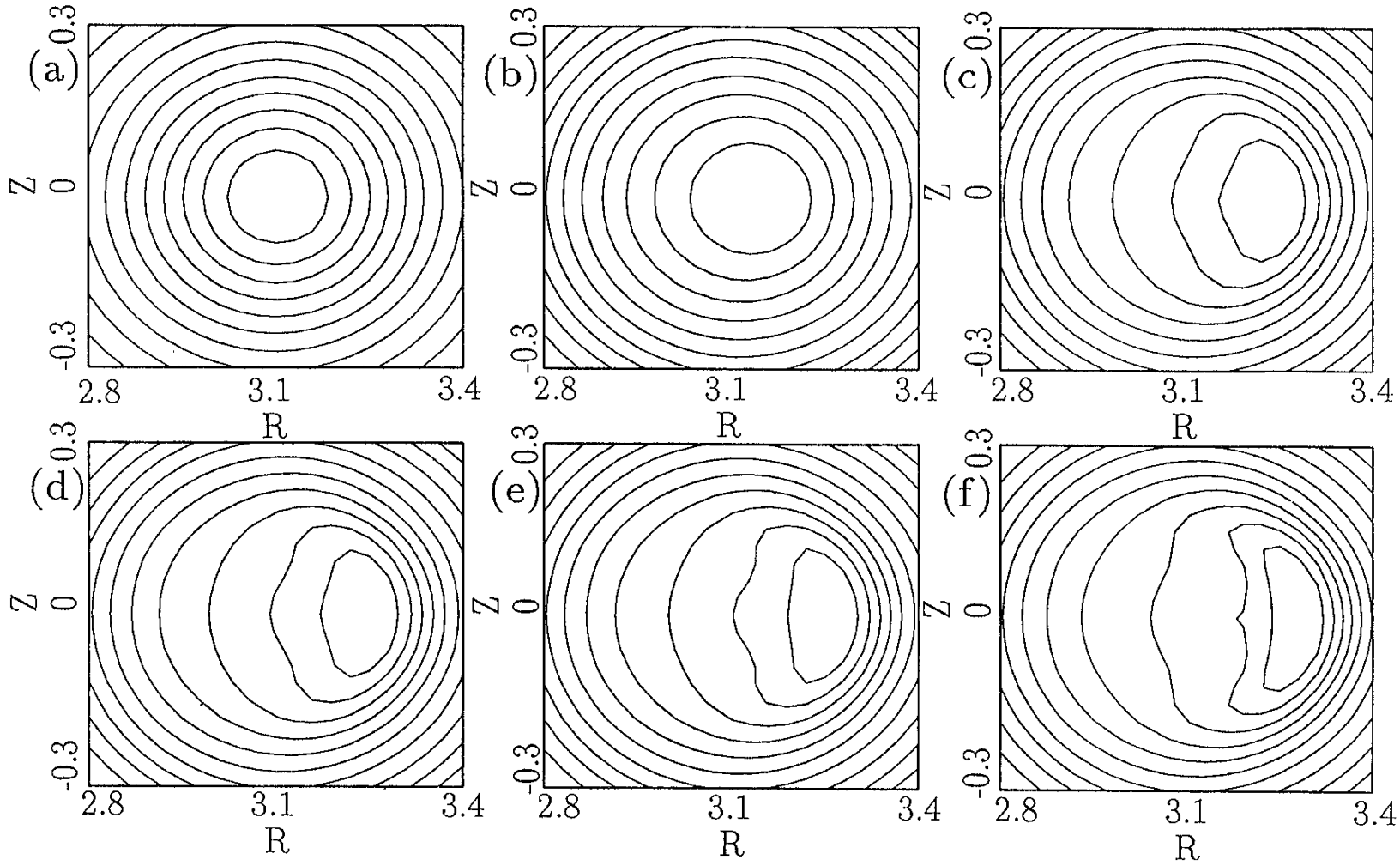

Figure 3

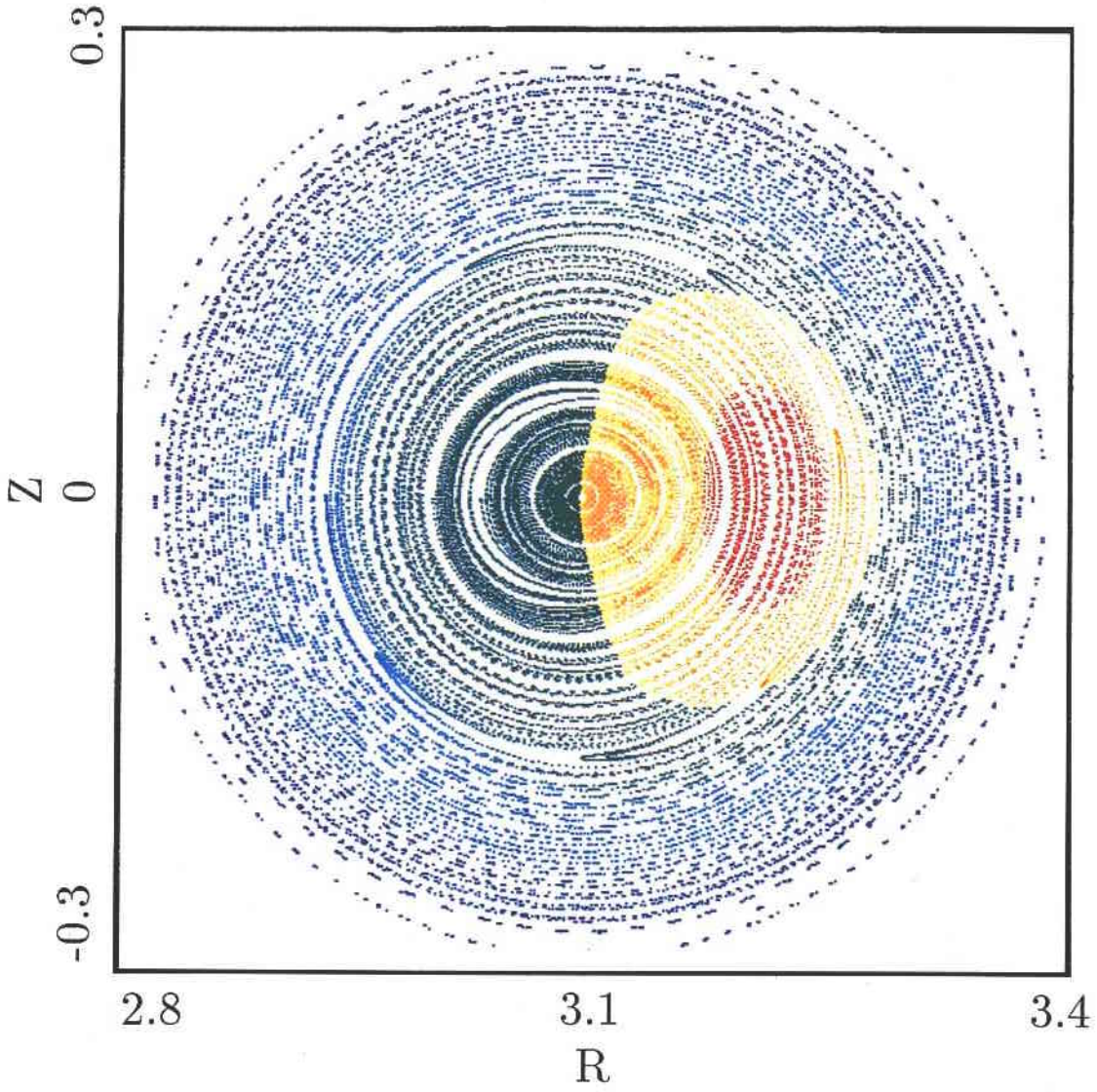

Figure 4

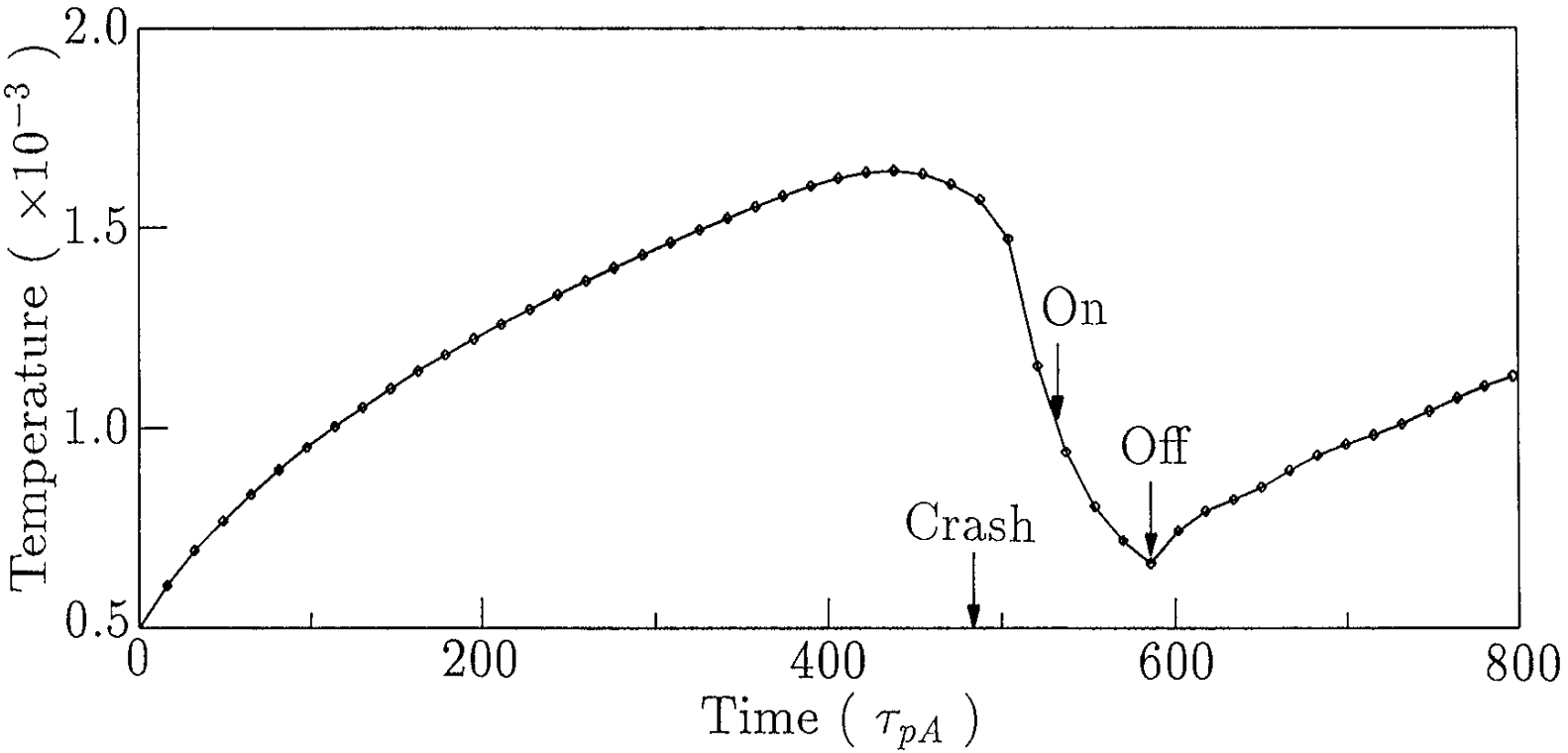
2.0
1.5
1.0
0.5
Temperature ($\times 10^{-3}$)
On
Off
Crash
0
200
400
600
800
Time (τ_{pA})

Figure 5

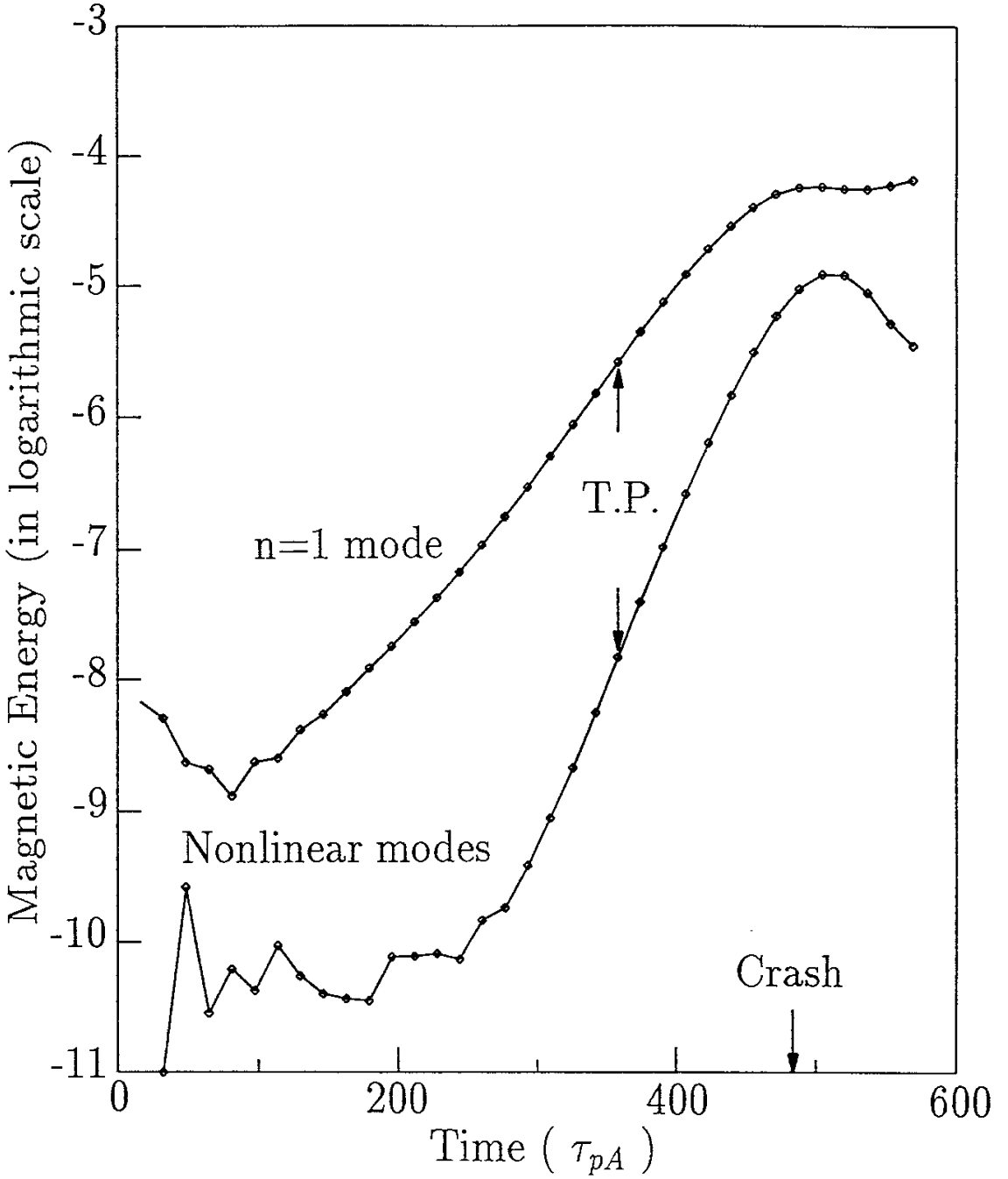
-3
-4
-5
-6
-7
-8
-9
-10
-11
Magnetic Energy (in logarithmic scale)
n=1 mode
T.P.
Nonlinear modes
Crash
0
200
400
600
Time (τ_{pA})

Figure 6-(a)

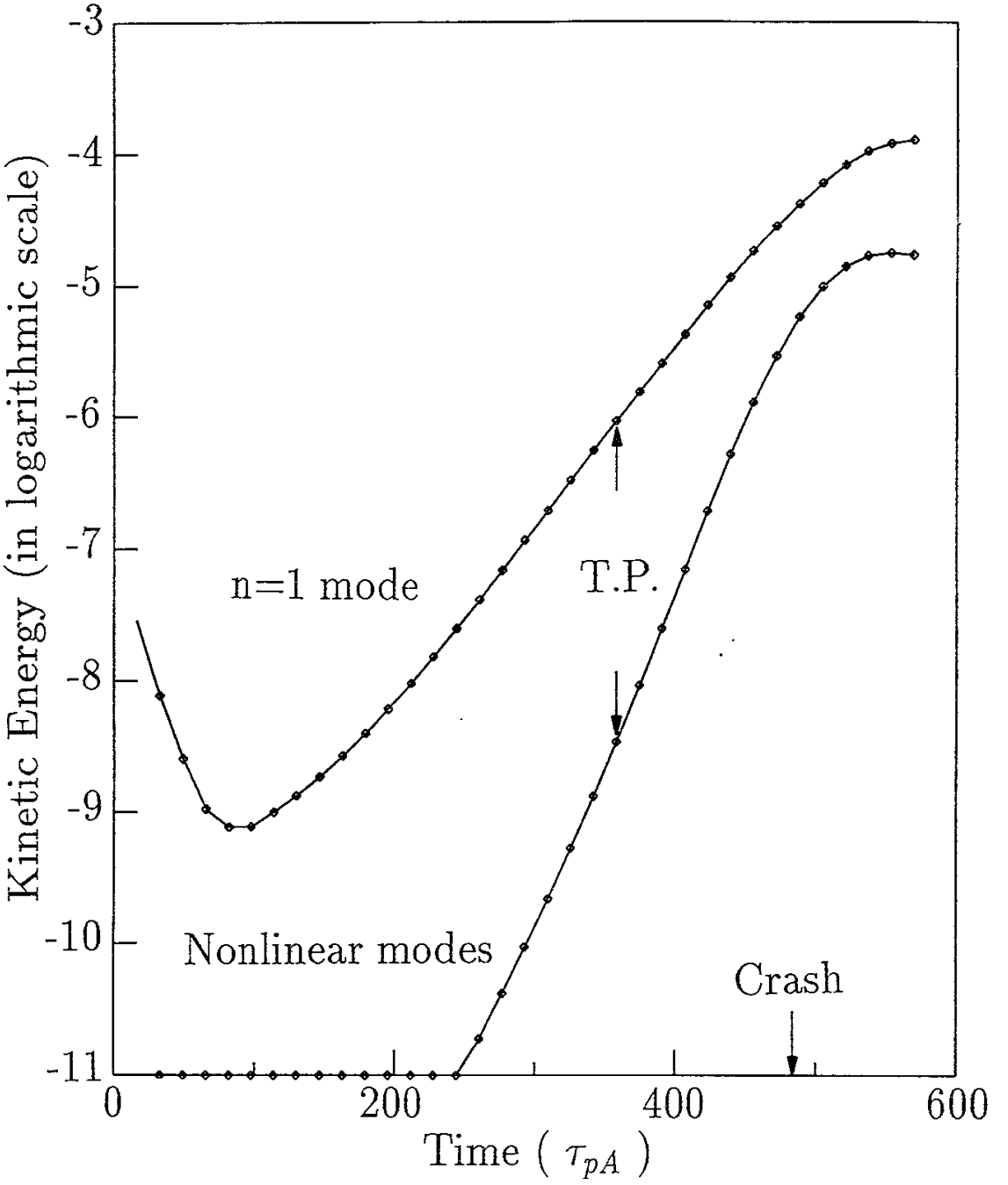
-3
-4
-5
-6
-7
-8
-9
-10
-11
Kinetic Energy (in logarithmic scale)
n=1 mode
T.P.
Nonlinear modes
Crash
0
200
400
600
Time (τ_{pA})

Figure 6-(b)

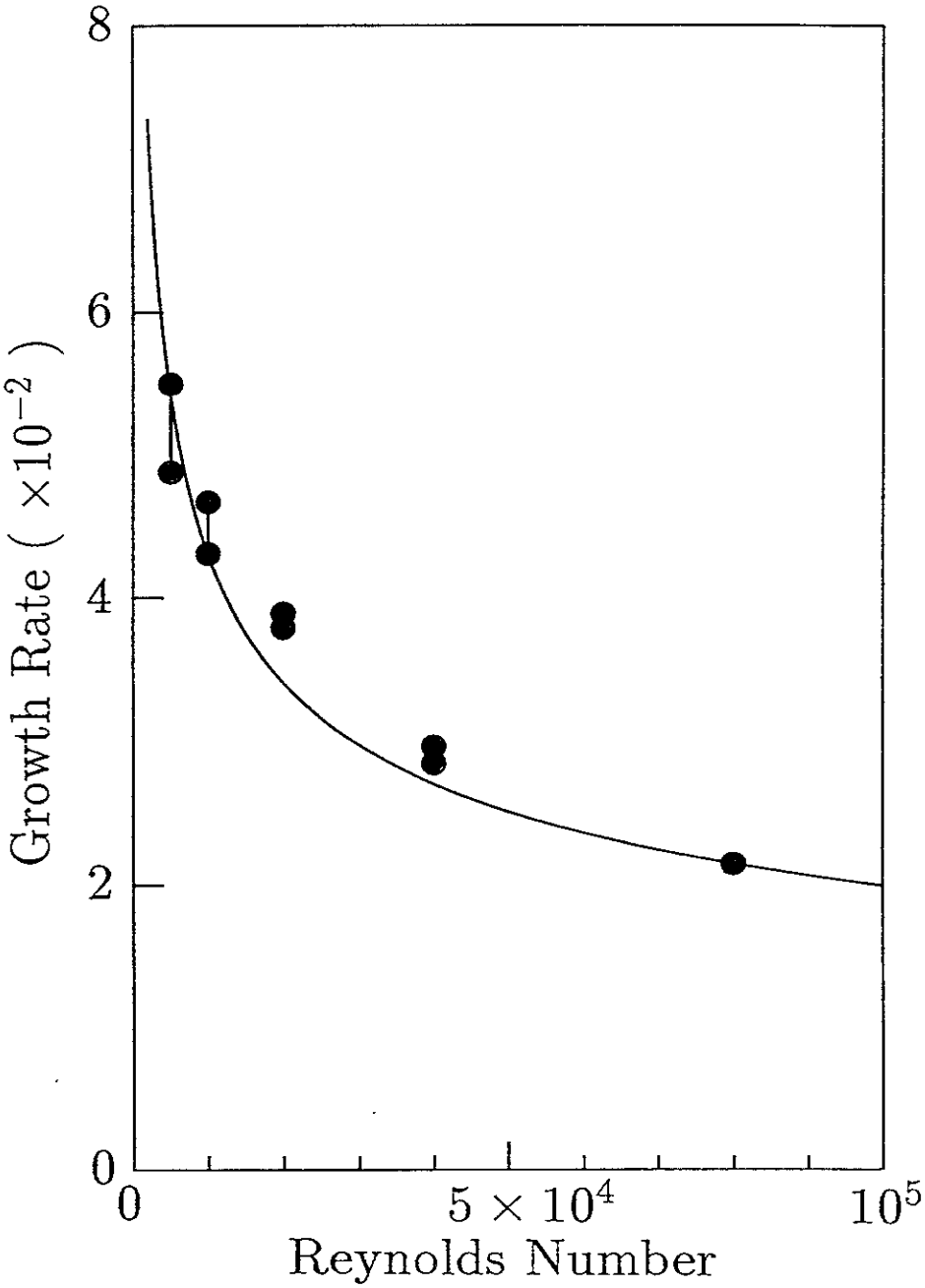
8
6
4
2
0
Growth Rate ($\times 10^{-2}$)
0
5×10^4
10^5
Reynolds Number

Figure 7

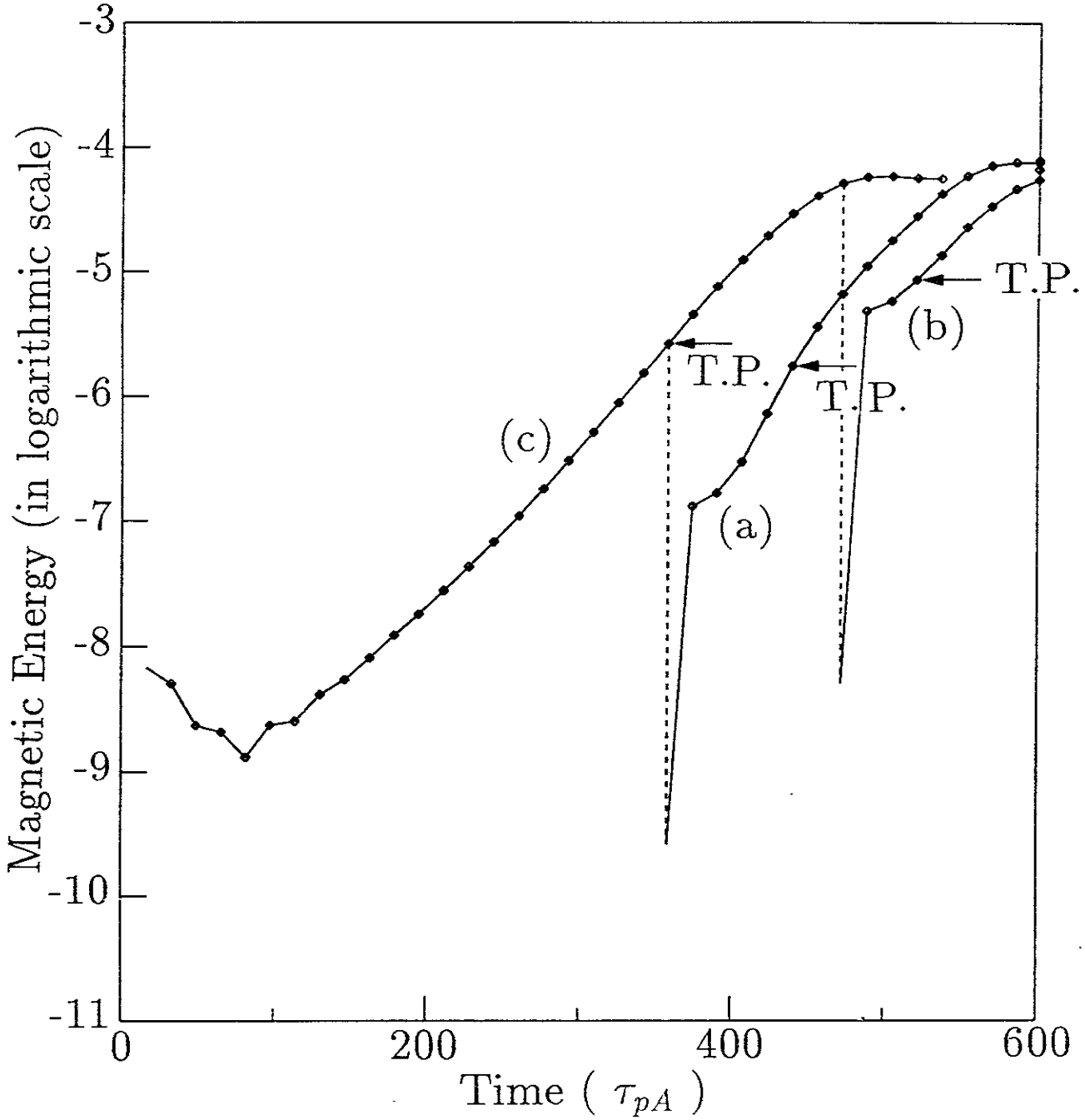
-3
-4
-5
-6
-7
-8
-9
-10
-11
0
200
400
600
Magnetic Energy (in logarithmic scale)
Time (τ_{pA})
(a)
(b)
(c)
T.P.
T.P.
T.P.
T.P.

Figure 8

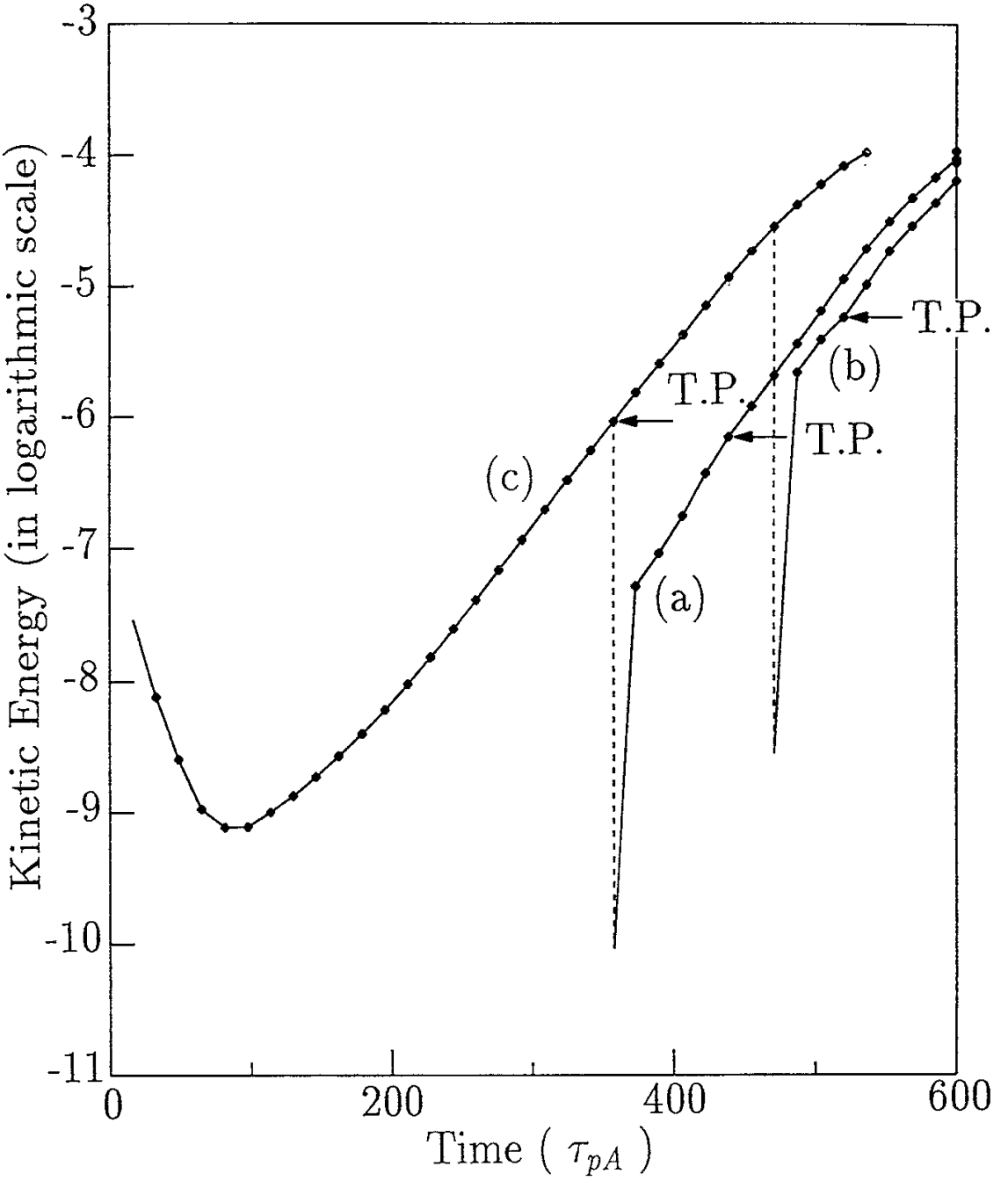
-3
-4
-5
-6
-7
-8
-9
-10
-11
0
200
400
600
Kinetic Energy (in logarithmic scale)
Time (τ_{pA})
T.P.
T.P.
T.P.
(a)
(b)
(c)

Figure 9

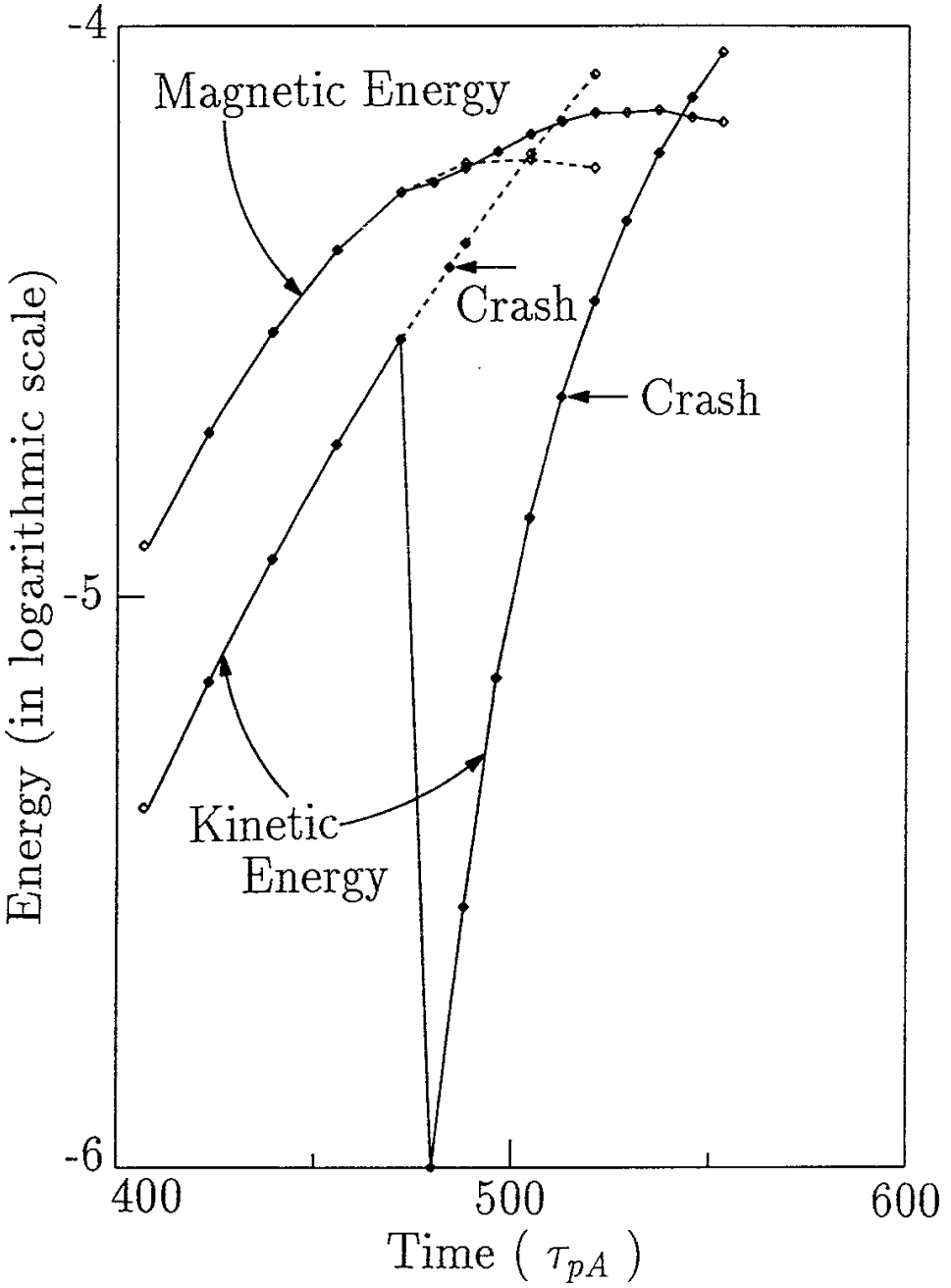
-4
-5
-6
Energy (in logarithmic scale)
Magnetic Energy
Crash
Crash
Kinetic
Energy
400
500
600
Time (τ_{pA})

Figure 10

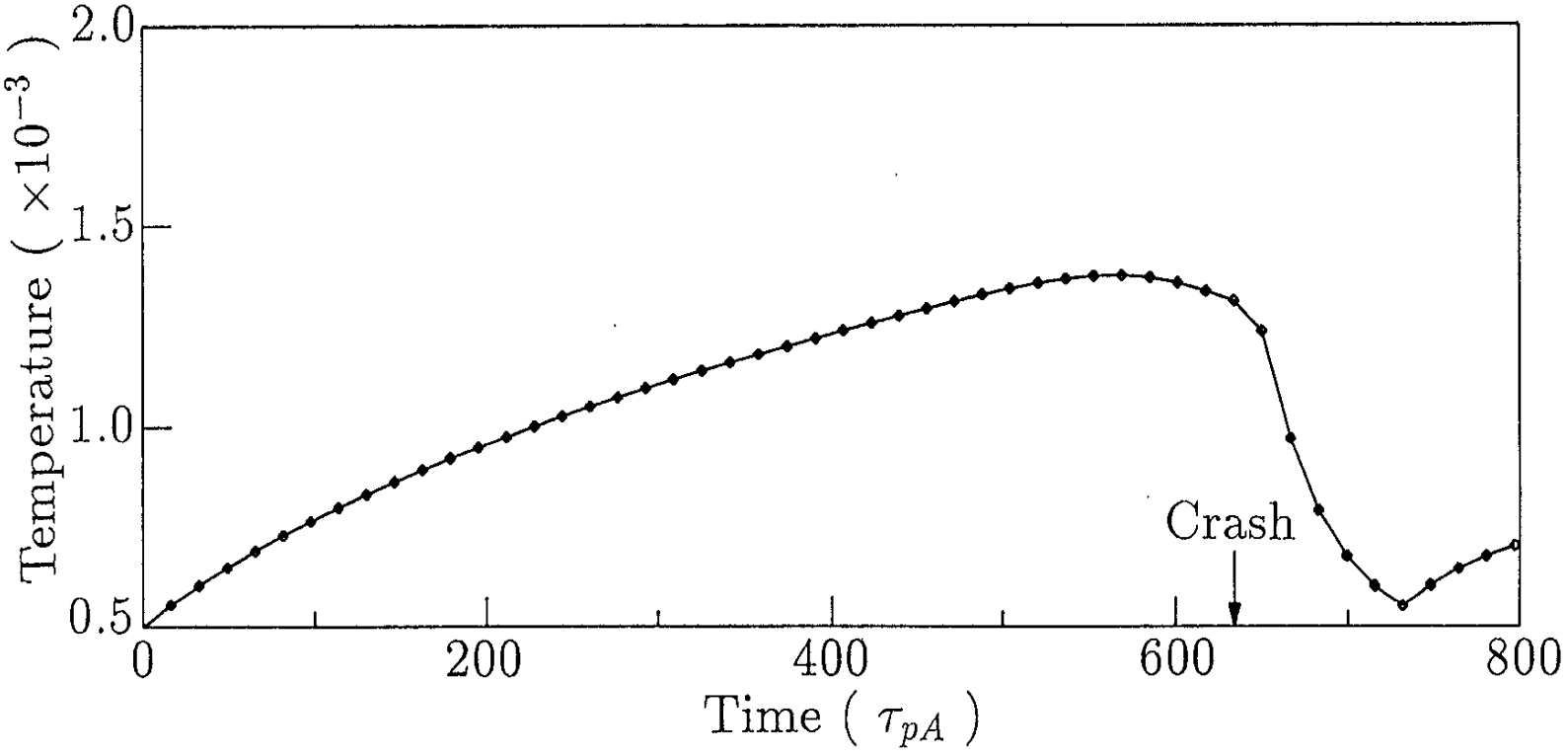
Temperature ($\times 10^{-3}$)
2.0
1.5
1.0
0.5
0
200
400
600
800
Time (τ_{pA})
Crash

Figure 11

Recent Issues of NIFS Series

NIFS-186 S. Morita, H. Yamada, H. Iguchi, K. Adati, R. Akiyama, H. Arimoto, M. Fujiwara, Y. Hamada, K. Ida, H. Idei, O. Kaneko, K. Kawahata, T. Kawamoto, S. Kubo, R. Kumazawa, K. Matsuoka, T. Morisaki, K. Nishimura, S. Okamura, T. Ozaki, T. Seki, M. Sakurai, S, Sakakibara, A. Sagara, C. Takahashi, Y. Takeiri, H. Takenaga, Y. Takita, K. Toi, K. Tsumori, K. Uchino, M. Ueda, T. Watari, I. Yamada, *A Role of Neutral Hydrogen in CHS Plasmas with Reheat and Collapse and Comparison with JIPP T-IIU Tokamak Plasmas* ; Sep. 1992

NIFS-187 K. Ioth, S.-I. Itoh, A. Fukuyama, M. Yagi and M. Azumi, *Model of the L-Mode Confinement in Tokamaks* ; Sep. 1992

NIFS-188 K. Itoh, A. Fukuyama and S.-I. Itoh, *Beta-Limiting Phenomena in High-Aspect-Ratio Toroidal Helical Plasmas*; Oct. 1992

NIFS-189 K. Itoh, S. -I. Itoh and A. Fukuyama, *Cross Field Ion Motion at Sawtooth Crash* ; Oct. 1992

NIFS-190 N. Noda, Y. Kubota, A. Sagara, N. Ohyabu, K. Akaishi, H. Ji, O. Motojima, M. Hashiba, I. Fujita, T. Hino, T. Yamashina, T. Matsuda, T. Sogabe, T. Matsumoto, K. Kuroda, S. Yamazaki, H. Ise, J. Adachi and T. Suzuki, *Design Study on Divertor Plates of Large Helical Device (LHD)* ; Oct. 1992

NIFS-191 Y. Kondoh, Y. Hosaka and K. Ishii, *Kernel Optimum Nearly-Analytical Discretization (KOND) Algorithm Applied to Parabolic and Hyperbolic Equations* : Oct. 1992

NIFS-192 K. Itoh, M. Yagi, S.-I. Itoh, A. Fukuyama and M. Azumi, *L-Mode Confinement Model Based on Transport-MHD Theory in Tokamaks* ; Oct. 1992

NIFS-193 T. Watari, *Review of Japanese Results on Heating and Current Drive* ; Oct. 1992

NIFS-194 Y. Kondoh, *Eigenfunction for Dissipative Dynamics Operator and Attractor of Dissipative Structure* ; Oct. 1992

NIFS-195 T. Watanabe, H. Oya, K. Watanabe and T. Sato, *Comprehensive Simulation Study on Local and Global Development of Auroral Arcs and Field-Aligned Potentials* ; Oct. 1992

NIFS-196 T. Mori, K. Akaishi, Y. Kubota, O. Motojima, M. Mushiaki, Y. Funato and Y. Hanaoka, *Pumping Experiment of Water on B and*

LaB_6 Films with Electron Beam Evaporator ; Oct., 1992

NIFS-197 T. Kato and K. Masai, *X-ray Spectra from Hinotori Satellite and Suprathermal Electrons* ; Oct. 1992

NIFS-198 K. Toi, S. Okamura, H. Iguchi, H. Yamada, S. Morita, S. Sakakibara, K. Ida, K. Nishimura, K. Matsuoka, R. Akiyama, H. Arimoto, M. Fujiwara, M. Hosokawa, H. Idei, O. Kaneko, S. Kubo, A. Sagara, C. Takahashi, Y. Takeiri, Y. Takita, K. Tsumori, I. Yamada and H. Zushi, *Formation of H-mode Like Transport Barrier in the CHS Heliotron / Torsatron* ; Oct. 1992

NIFS-199 M. Tanaka, *A Kinetic Simulation of Low-Frequency Electromagnetic Phenomena in Inhomogeneous Plasmas of Three-Dimensions* ; Nov. 1992

NIFS-200 K. Itoh, S.-I. Itoh, H. Sanuki and A. Fukuyama, *Roles of Electric Field on Toroidal Magnetic Confinement*, Nov. 1992

NIFS-201 G. Gnudi and T. Hatori, *Hamiltonian for the Toroidal Helical Magnetic Field Lines in the Vacuum*; Nov. 1992

NIFS-202 K. Itoh, S.-I. Itoh and A. Fukuyama, *Physics of Transport Phenomena in Magnetic Confinement Plasmas*; Dec. 1992

NIFS-203 Y. Hamada, Y. Kawasumi, H. Iguchi, A. Fujisawa, Y. Abe and M. Takahashi, *Mesh Effect in a Parallel Plate Analyzer*; Dec. 1992

NIFS-204 T. Okada and H. Tazawa, *Two-Stream Instability for a Light Ion Beam -Plasma System with External Magnetic Field;* Dec. 1992

NIFS-205 M. Osakabe, S. Itoh, Y. Gotoh, M. Sasao and J. Fujita, *A Compact Neutron Counter Telescope with Thick Radiator (Cotetra) for Fusion Experiment*; Jan. 1993

NIFS-206 T. Yabe and F. Xiao, *Tracking Sharp Interface of Two Fluids by the CIP (Cubic-Interpolated Propagation) Scheme*, Jan. 1993

NIFS-207 A. Kageyama, K. Watanabe and T. Sato, *Simulation Study of MHD Dynamo : Convection in a Rotating Spherical Shell*; Feb. 1993

NIFS-208 M. Okamoto and S. Murakami, *Plasma Heating in Toroidal Systems*; Feb. 1993

NIFS-209 K. Masai, *Density Dependence of Line Intensities and Application to Plasma Diagnostics*; Feb. 1993

NIFS-210 K. Ohkubo, M. Hosokawa, S. Kubo, M. Sato, Y. Takita and T. Kuroda,

R&D of Transmission Lines for ECH System ; Feb. 1993

NIFS-211 A. A. Shishkin, K. Y. Watanabe, K. Yamazaki, O. Motojima, D. L. Grekov, M. S. Smirnova and A. V. Zolotukhin, *Some Features of Particle Orbit Behavior in LHD Configurations*; Mar. 1993

NIFS-212 Y. Kondoh, Y. Hosaka and J.-L. Liang, *Demonstration for Novel Self-organization Theory by Three-Dimensional Magnetohydrodynamic Simulation*; Mar. 1993

NIFS-213 K. Itoh, H. Sanuki and S.-I. Itoh, *Thermal and Electric Oscillation Driven by Orbit Loss in Helical Systems*; Mar. 1993

NIFS-214 T. Yamagishi, *Effect of Continuous Eigenvalue Spectrum on Plasma Transport in Toroidal Systems*; Mar. 1993

NIFS-215 K. Ida, K. Itoh, S.-I.Itoh, Y. Miura, JFT-2M Group and A. Fukuyama, *Thickness of the Layer of Strong Radial Electric Field in JFT-2M H-mode Plasmas*; Apr. 1993

NIFS-216 M. Yagi, K. Itoh, S.-I. Itoh, A. Fukuyama and M. Azumi, *Analysis of Current Diffusive Ballooning Mode*; Apr. 1993

NIFS-217 J. Guasp, K. Yamazaki and O. Motojima, *Particle Orbit Analysis for LHD Helical Axis Configurations* ; Apr. 1993

NIFS-218 T. Yabe, T. Ito and M. Okazaki, *Holography Machine HORN-1 for Computer-aided Retrieve of Virtual Three-dimensional Image* ; Apr. 1993

NIFS-219 K. Itoh, S.-I. Itoh, A. Fukuyama, M. Yagi and M. Azumi, *Self-sustained Turbulence and L-Mode Confinement in Toroidal Plasmas* ; Apr. 1993

NIFS-220 T. Watari, R. Kumazawa, T. Mutoh, T. Seki, K. Nishimura and F. Shimpo, *Applications of Non-resonant RF Forces to Improvement of Tokamak Reactor Performances Part I: Application of Ponderomotive Force* ; May 1993

NIFS-221 S.-I. Itoh, K. Itoh, and A. Fukuyama, *ELMy-H mode as Limit Cycle and Transient Responses of H-modes in Tokamaks* ; May 1993

NIFS-222 H. Hojo, M. Inutake, M. Ichimura, R. Katsumata and T. Watanabe, *Interchange Stability Criteria for Anisotropic Central-Cell Plasmas in the Tandem Mirror GAMMA 10 ;* May 1993

NIFS-223 K. Itoh, S.-I. Itoh, M. Yagi, A. Fukuyama and M. Azumi, *Theory of Pseudo-Classical Confinement and Transmutation to L-Mode;* May

1993

NIFS-224 M. Tanaka, *HIDENEK: An Implicit Particle Simulation of Kinetic-MHD Phenomena in Three-Dimensional Plasmas;* May 1993

NIFS-225 H. Hojo and T. Hatori, *Bounce Resonance Heating and Transport in a Magnetic Mirror;* May 1993

NIFS-226 S.-I. Iton, K. Itoh, A. Fukuyama, M. Yagi, *Theory of Anomalous Transport in H-Mode Plasmas;* May 1993

NIFS-227 T. Yamagishi, *Anomalous Cross Field Flux in CHS ;* May 1993

NIFS-228 Y. Ohkouchi, S. Sasaki, S. Takamura, T. Kato, *Effective Emission and Ionization Rate Coefficients of Atomic Carbons in Plasmas;* June 1993

NIFS-229 K. Itoh, M. Yagi, A. Fukuyama, S.-I. Itoh and M. Azumi, *Comment on 'A Mean Field Ohm's Law for Collisionless Plasmas;* June 1993

NIFS-230 H. Idei, K. Ida, H. Sanuki, H. Yamada, H. Iguchi, S. Kubo, R. Akiyama, H. Arimoto, M. Fujiwara, M. Hosokawa, K. Matsuoka, S. Morita, K. Nishimura, K. Ohkubo, S. Okamura, S. Sakakibara, C. Takahashi, Y. Takita, K. Tsumori and I. Yamada, *Transition of Radial Electric Field by Electron Cyclotron Heating in Stellarator Plasmas;* June 1993

NIFS-231 H.J. Gardner and K. Ichiguchi, *Free-Boundary Equilibrium Studies for the Large Helical Device,* June 1993

NIFS-232 K. Itoh, S.-I. Itoh, A. Fukuyama, H. Sanuki and M. Yagi, *Confinement Improvement in H-Mode-Like Plasmas in Helical Systems,* June 1993

NIFS-233 R. Horiuchi and T. Sato, *Collisionless Driven Magnetic Reconnection,* June 1993

NIFS-234 K. Itoh, S.-I. Itoh, A. Fukuyama, M. Yagi and M. *Azumi, Prandtl Number of Toroidal Plasmas;* June 1993

NIFS-235 S. Kawata, S. Kato and S. Kiyokawa , *Screening Constants for Plasma;* June 1993

NIFS-236 A. Fujisawa and Y. Hamada, *Theoretical Study of Cylindrical Energy Analyzers for MeV Range Heavy Ion Beam Probes;* July 1993

NIFS-237 N. Ohyabu, A. Sagara, T. Ono, T. Kawamura and O. Motojima, *Carbon Sheet Pumping;* July 1993